Available online at www.sciencedirect.com

ScienceDirect

Ceramics International 40 (2014) 929–933

CERAMICS INTERNATIONAL

www.elsevier.com/locate/ceramint

Effects of Sr/Ti ratio on the microstructure and energy storage properties of nonstoichiometric $SrTiO_3$ ceramics

Zhijian Wang, Minghe Cao*, Zhonghua Yao*, Guangyao Li, Zhe Song, Wei Hu, Hua Hao, Hanxing Liu, Zhiyong Yu

State Key Laboratory of Advanced Technology for Materials Synthesis and Processing, Wuhan University of Technology, Wuhan 430070, Hubei, PR China

Received 18 May 2013; received in revised form 25 June 2013; accepted 25 June 2013
Available online 29 June 2013

Abstract

Effects of nonstoichiometric $SrTiO_3$ ceramics have been investigated in the range of Sr/Ti=0.994–1.004. A cubic perovskite structure is maintained at all compositions without any secondary phase. Grain size increases at the beginning and then decreases with increasing Sr/Ti ratio. The highest breakdown strength and energy density are obtained at Sr/Ti=0.996, 283 kV/cm and 1.21 J/cm^3, respectively, which are higher than that of stoichiometric $SrTiO_3$ ceramic (210 kV/cm of breakdown strength, 0.7 J/cm^3 of energy density). Sr/Ti > 1 ST ceramics are prone to semiconductivity process. Among them, the ST ceramic at Sr/Ti=1.004 has the highest permittivity, 2455.

Keywords: B. Nonstoichiometry; C. Energy storage property; D. $SrTiO_3$ ceramic; Microstructure

1. Introduction

As quantum paraelectrics, $SrTiO_3$ (ST) ceramic has been developed for a wide range of applications in energy density capacitors because of its high permittivity, high breakdown strength and favorable bias stability. In general, energy storage density of ceramics is given by the following equation [1]:

$$W = \int_0^{E_b} EdP \tag{1}$$

where P and E are the polarization and the electric field, E_b is the breakdown strength. Thus, the energy storage density can be evaluated by integrating the area between the polarization axis and the discharge curve in the P–E hysteresis loops. For linear dielectrics, Eq. (1) can be converted into the following equation [2]:

$$W = \frac{1}{2}\varepsilon_r\varepsilon_0 E_b^2 \tag{2}$$

where ε_r is the relative permittivity and ε_0 is the permittivity of free space (8.85×10^{-12} F/m). As can be seen in Eqs. (1) and (2), energy density is influenced by permittivity and breakdown strength, particularly breakdown strength. Hence, increasing breakdown strength will be more helpful for improving energy density.

Burn [2] indicated that at the maximum fields, energy storage in the strontium titanate material was about 30% higher than that in the barium titanate ceramic. To improve its permittivity at room temperature, rare earth Nd^{3+} was selected to dope in this system and high permittivity ceramics were obtained [3,4]. Also it was proved that doping by other cations with small ionic radius could improve the permittivity, such as Ba^{2+}, Mn^{2+}, Bi^{3+} and trivalent rare earth (RE^{3+}) [5–14], however the breakdown strength decreased [3]. Thus, these were not beneficial to energy density. Although energy density is related to permittivity and breakdown strength, it is well-known that the maximum energy storage is not obtained in high dielectric constant materials but

*Corresponding authors. Tel.: +86 27 87885812; fax: +86 27 87885813.
E-mail addresses: caominghe@whut.edu.cn (M. Cao), yaozhhua@whut.edu.cn (Z. Yao).

0272-8842/$ - see front matter © 2013 Elsevier Ltd and Techna Group S.r.l. All rights reserved.
http://dx.doi.org/10.1016/j.ceramint.2013.06.088

in those materials which display intermediate dielectric constant and the highest ultimate breakdown voltages [15]. For the linear-dielectric ST ceramic, energy density can be calculated by Eq. (2), which is square relation with breakdown strength. Hence, increasing breakdown strength will be more helpful for energy density. It is well known that the breakdown strength is mainly affected by density and grain size of dielectric ceramics [16]. Though the A- or B-site substitution by some cations can obtain small grain-size ceramic, they will change the crystal lattice, even lead to low breakdown strength. Several low-melting point glasses as additives can significantly reduce the grain size and improve the breakdown strength, but also reduce the permittivity [17,18]. Therefore, reducing grain size and/or increasing permittivity will efficiently improve the energy density of ST ceramic.

Tkach [19] considered that the change of Sr/Ti ratio can result in the changes of grain size and dielectric properties of ST ceramics. And in the certain range of Sr/Ti ratio, there was no impurity phase in the ceramics which exhibited the same structure as stoichiometric ST ceramic. Guo [20] demonstrated the existence of ferroelectric polarization and superparamagnetism in the nonstoichiometry $SrTiO_3$, which increased with the degree of nonstoichiometry. However, the grain size had no obvious difference from stoichiometry ST ceramic, indicating that grain size in nonstoichiometry ST ceramics was not only influenced by Sr/Ti, but also by preparation method. In any case, nonstoichiometry has certain influences on the microstructure of ceramics, which also observed on other materials [21–23]. In this paper, the microstructure, electrical properties and energy storage performance of the ST ceramics with the slight change of Sr/Ti ratio were intensively studied.

2. Experimental

The ceramics studied were prepared by conventional solid-state reactions. The starting materials, high purity $SrCO_3$(> 99.0%) and TiO_2(> 99.0%) were mixed according to the composition, $Sr_{1\pm x}TiO_3$ (x=0, 0.002, 0.004, −0.002, −0.004, and −0.006). After ball-milled in alcohol for 24 h, the slurry was dried, then calcined in a closed environment at 1150 °C for 2 h. The calcined powder was ball milled and dried again to obtain homogeneous powder. Pellets of 12 mm in diameter and about 0.5 mm thickness were uniaxially pressed at 200 MPa using 5% PVA binder. Slow heating at 600 °C for 2 h burned out the binder. The samples were sintered at 1440 °C for 2 h in air. The relative densities of all the sintered samples are more than 97%.

The crystalline structure of sintered samples was analyzed by an X-ray diffractometer (XRD, PANalytical X'Pert PRO). The microstructure of ceramics was observed using a scanning electron microscope (SEM, Hitachi S3400).

For the electrical measurements, the sintered ceramics were polished to 0.3 mm in thickness and coated with silver electrodes on both faces. The dielectric properties and complex impedance spectra were measured by a precision impedance analyzer (Agilent 4980A). The breakdown strength and *P–E* hysteresis loop were determined by a DC bias source on a ferroelectric test system (Radiant RT66A), and the energy storage density was calculated from the *P–E* hysteresis loop obtained by Eq. (1). For each composition, at least 8 samples were measured to obtain average breakdown strength.

3. Results and discussion

Fig. 1 shows the XRD patterns of the sintered ST samples. A cubic symmetry was detected by XRD analysis for all compositions without any secondary phase. All of the XRD patterns were identical to the stoichiometric ST ceramic. No systematic variation of the lattice parameter was observed.

The SEM micrographs of the ceramics sintered at 1440 °C for 2 h, shown in Fig. 2 reveal rather dense microstructures for all the samples, and obvious difference in grain size for nonstoichiometric ST ceramics with different Sr/Ti ratios. Fig. 3 shows the change of grain size for the samples with different Sr/Ti ratios. Large grain size of sintered samples was obtained at Sr/Ti = 1. the grain size at Sr/Ti > 1 decreased with increasing Sr/Ti ratio, however the grain size dramatically decreased at Sr/Ti < 1, which was different from those in the previously reported cases [19]. This can be ascribed to different vacancies probably by the preparation method and/or different Sr/Ti ratios. The resistivity of all the sintered samples was shown in Fig. 4. The low resistivity was obtained at nonstoichiometric ST ceramics, among them the resistivity of Sr/Ti > 1 samples was lower than that of Sr/Ti < 1 samples. More remarkable, Sr/Ti = 1.004 sample with blue color had the lowest value of 3.2×10^9 Ω cm, meaning the semi-conductive process and the emergence of Ti^{3+}.

The room-temperature dielectric properties of nonstoichiometric ST ceramics at 1 kHz are shown in Table 1. All the samples exhibit the approximate permittivity and dielectric loss except Sr/Ti = 1.004 because of its low resistivity shown in Fig. 3. However the energy densities of different Sr/Ti ratio samples are evidently different from each other, which should be attributed to the variant breakdown strength (BDS), shown

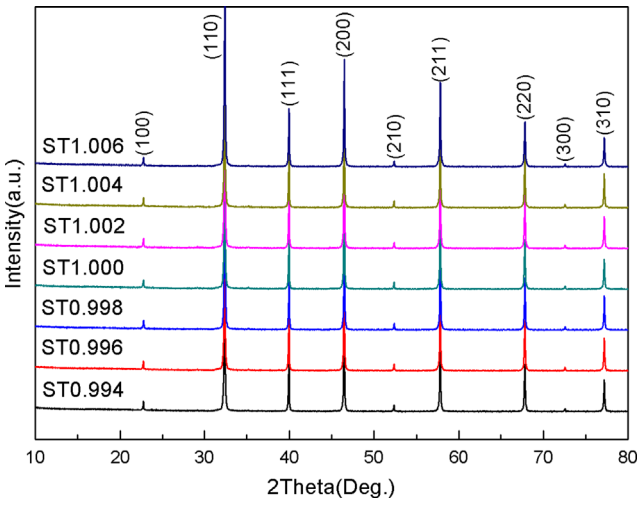

Fig. 1. XRD patterns of sintered nonstoichiometric ST ceramics.

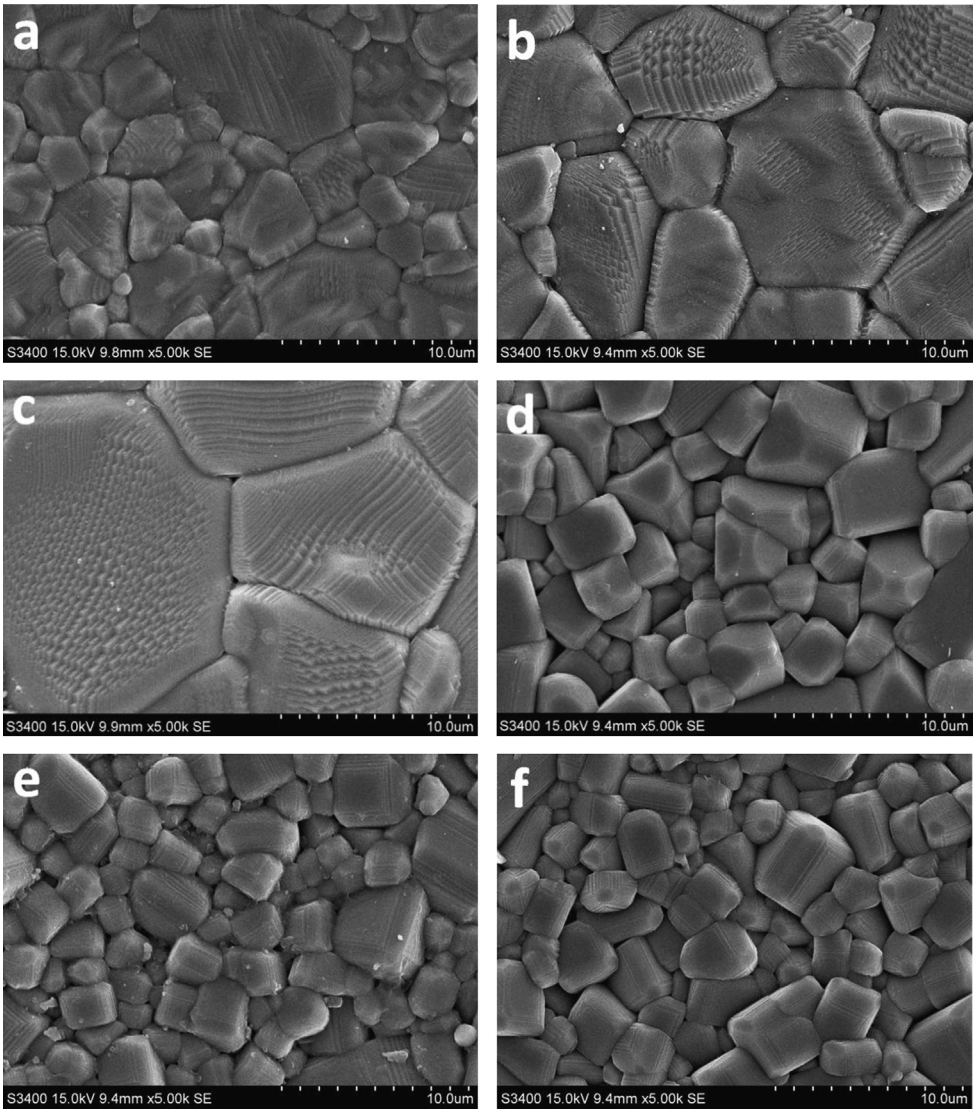

Fig. 2. SEM micrographs of nonstoichiometric ST ceramics sintered at 1440 °C for 2 h. (a) ST1.004, (b) ST1.002, (c) ST1.000, (d) ST0.998, (e) ST0.996, and (f) ST0.994.

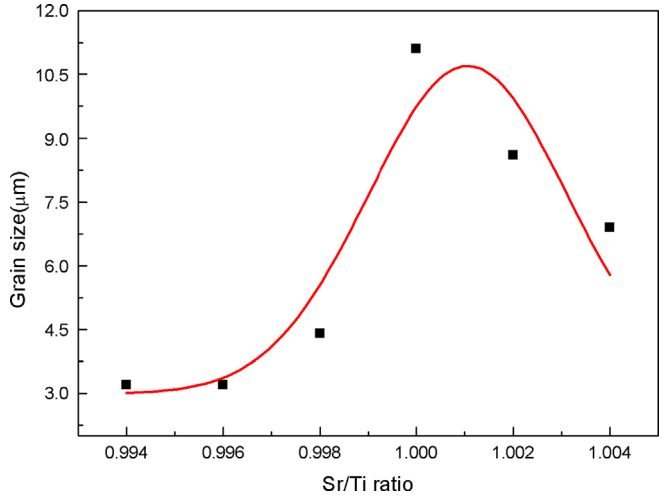

Fig. 3. Grain sizes of nonstoichiometric ST ceramics sintered at 1440 °C for 2 h.

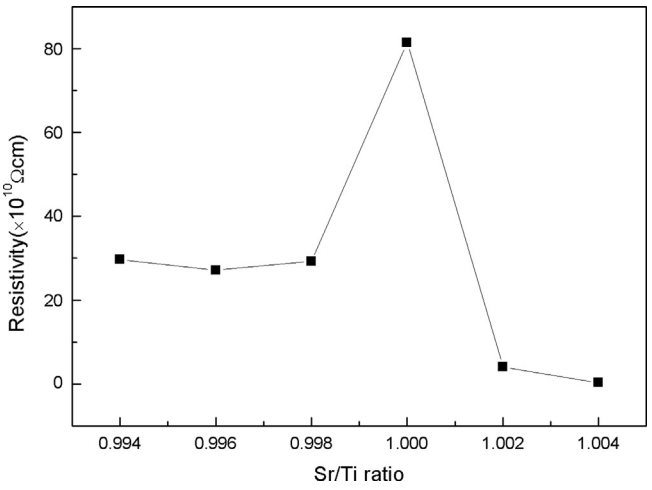

Fig. 4. Resistivity of nonstoichiometric ST ceramics sintered at 1440 °C for 2 h.

in Fig. 5. The high breakdown strengths (BDS) and energy densities have been obtained in the range of Sr/Ti < 1 because of their smaller grain sizes, which greatly affect the BDS [16]. Although the grain sizes of the sample at Sr/Ti = 1.002 are smaller than that at Sr/Ti = 1.000, the BDS at Sr/Ti = 1.002 is lower, which may be due to the lower resistivity.

Fig. 6 shows the complex impedance spectra measured at 420 °C for the specimens with different Sr/Ti ratios. It can be seen that the complex impedance plots of Sr/Ti≥1 ceramics display only one suppressed semicircle which can be associated with a strong overlap of two semicircles due to similar relaxation time constant τ of the two relaxation processes. And the ceramics at Sr/Ti < 1 display two semicircles, meaning that grain boundary has played an important part in the complex impedance spectra. The inset in Fig. 6 shows an equivalent circuit for the Sr/Ti < 1 ceramics system, where the circuit elements R_g–C_g and R_{gb}–C_{gb} represent the contributions from the grain and grain boundary, respectively. The fitting values of the R_g, C_g, R_{gb} and C_{gb} are shown in Table 2. The relaxation time τ is defined as:

$$\tau = RC \tag{3}$$

The relaxation time of grain (τ_g) and grain boundary (τ_{gb}) are given in Table 2. The ratio between the grain boundary (ρ_{gb}) and grain (ρ_g) is given by the following equation:

$$\rho_{gb}/\rho_g = \tau_{gb}/\tau_g \tag{4}$$

The ρ_{gb}/ρ_g and $R_{gb}/(R_{gb}+R_g)$ were given in Fig. 7. As seen from the figure, the ceramic at Sr/Ti = 0.996 exhibited the higher ρ_{gb}/ρ_g and $R_{gb}/(R_{gb}+R_g)$ ratios than the other compositions, indicating that grain boundary showed great contribution to the insulating properties. Furthermore, the large electrical difference between grain and grain boundary in Sr/Ti = 0.996 ceramic may be the main cause of higher BDS.

Table 1
The room-temperature dielectric properties of nonstoichiometric ST ceramics at 1 kHz.

Sr/Ti ratio	1.004	1.002	1.000	0.998	0.996	0.994
ε_r	2455	317	295	349	299	268
tan δ	0.13	0.007	0.002	0.006	0.001	0.003

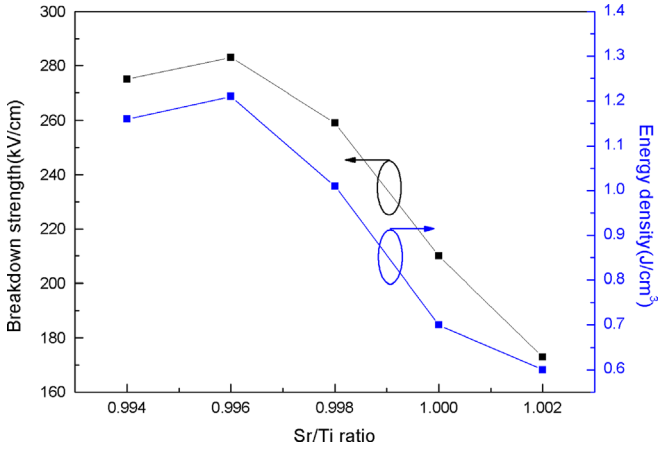

Fig. 5. Breakdown strengths and energy densities of nonstoichiometric ST ceramics.

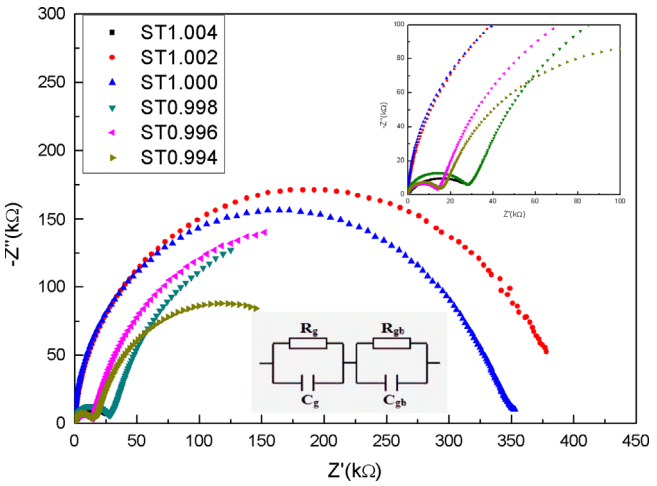

Fig. 6. The complex impedance spectra measured at 420 °C for the specimens with different Sr/Ti ratios.

Table 2
The equivalent parameters at 420 °C of different electrical regions for ST ceramics at Sr/Ti < 1.

Sample	R_g(Ω)	C_g(pF)	τ_g(ns)	R_{gb}(Ω)	C_{gb}(pF)	τ_{gb}(ns)
ST0.998	29,271	167	4888	214,450	34,197	7,333,547
ST0.996	14,566	145	2112	230,150	23,086	5,313,243
ST0.994	16,451	152	2501	160,010	22,870	3,659,429

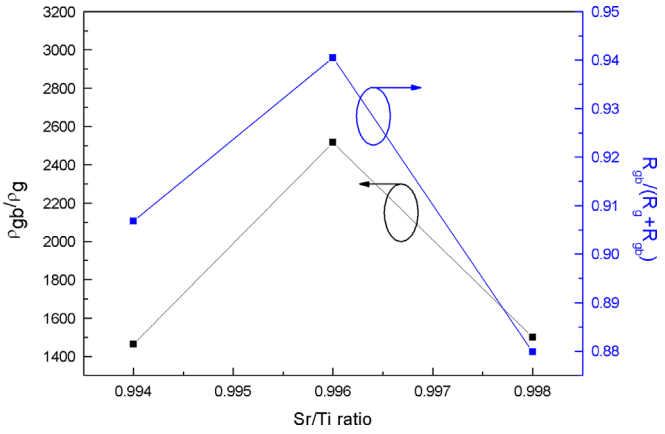

Fig. 7. The ρ_{gb}/ρ_g and $R_{gb}/(R_{gb}+R_g)$ ratios at 420 °C for ST ceramics at Sr/Ti < 1.

4. Conclusions

The microstructure, dielectric, and energy storage properties of nonstoichiometric ST ceramics were intensively investigated. With the change of Sr/Ti ratio, its effects were significant. With the increase of Sr/Ti ratio, the grain size increased at the beginning and then decreased. The highest

breakdown strength and energy density were obtained at the sample of Sr/Ti = 0.996 with smaller grain size, 283 kV/cm and 1.21 J/cm^3, respectively. ST ceramics at Sr/Ti > 1 were prone to semi-conductivity process.

Acknowledgments

This work was supported by the Key program of Natural Science Foundation of China (No.50932004), International Science and Technology Cooperation Program of China (2011DFA52680), Natural Science Foundation of China (No.51102189), the program for New Century Excellent Talents in University (No.NCET-11-0685).

References

[1] N.H. Fletcher, A.D. Hilton, et al., Optimization of energy storage density in ceramic capacitors, Journal of Physics D: Applied Physics 29 (1996) 253–258.
[2] I. Burn, D.M. Smyth, Energy storage in Ceramic Dielectrics, Journal of Materials Science 7 (1972) 339–343.
[3] Z. Shen, W. Luo, Y. Li, et al., Electrical hetero-structure of $Nd_{0.1}Sr_{0.9}TiO_3$ ceramic for energy storage applications, Journal of Materials Science: Materials in Electronics 24 (2013) 607–612.
[4] Z. Shen, Y. Li, W. Luo, et al., Structure and dielectric properties of $Nd_xSr_{1-x}TiO_3$ ceramics for energy storage application, Journal of Materials Science: Materials in Electronics 24 (2013) 704–710.
[5] R.P. Wang, Y. Inaguma, M. Itoh, Dielectric properties and phase transition mechanisms in $Sr_{1-x}Ba_xTiO_3$ solid solution at low doping concentration, Materials Research Bulletin 36 (2001) 1693–1701.
[6] A. Tkach, P.M. Vilarinho, A.L. Kholkin, Nonlinear dc electric-field dependence of the dielectric permittivity and cluster polarization of $Sr_{1-x}Mn_xTiO_3$ ceramics, Journal of Applied Physics 101 (2007) 084110.
[7] A. Tkach, P.M. Vilarinho, A.L. Kholkin, et al., Broad-band dielectric spectroscopy analysis of relaxational dynamics in Mn-doped $SrTiO_3$ ceramics, Physical Review B 73 (2006) 10411310.
[8] A. Tkach, P.M. Vilarinho, A.L. Kholkin, Polar behavior in Mn-doped $SrTiO_3$ ceramics, Applied Physics Letters 86 (2005) 17290217.
[9] A. Chen, Z. Yu, J. Scott, et al., Dielectric polarization processes in Bi:$SrTiO_3$, Journal of Physics and Chemistry of Solids 61 (2000) 191–196.
[10] C. Ang, Z. Yu, L.E. Cross, Oxygen-vacancy-related low-frequency dielectric relaxation and electrical conduction in Bi:$SrTiO_3$, Physical Review B 62 (2000) 228–236.
[11] Y. Zhi, A. Chen, P.M. Vilarinho, et al., Dielectric relaxation behavior of Bi:$SrTiO_3$: I. The low temperature permittivity peak, Journal of the European Ceramic Society 18 (1998) 1613–1619.
[12] Z. Yu, C. Ang, L.E. Cross, Oxygen-vacancy-related dielectric anomalies in La: $SrTiO_3$, Applied Physics Letters 74 (1999) 3044–3046.
[13] X. Wang, Q. Hu, L. Li, et al., Effect of Pr substitution on structural and dielectric properties of $SrTiO_3$, Journal of Applied Physics 112 (2012) 0441064.
[14] L. Fang, W. Dong, F. Zheng, et al., Effects of Gd substitution on microstructures and low temperature dielectric relaxation behaviors of $SrTiO_3$ ceramics, Journal of Applied Physics 112 (2012) 0341143.
[15] G.R. Love, Energy storage in ceramic dielectrics, Journal of the American Ceramic Society 73 (1990) 323–328.
[16] A. Young, G. Hilmas, S.C. Zhang, et al., Effect of liquid-phase sintering on the breakdown strength of barium titanate, Journal of the American Ceramic Society 90 (2007) 1504–1510.
[17] G. Zhao, Y. Li, H. Liu, et al., Effect of SiO_2 additives on the microstructure and energy storage density of $SrTiO_3$ ceramics, Journal of Ceramic Processing Research 13 (2012) 310–314.
[18] K. Chen, Y. Pu, N. Xu, et al., Effects of SrO–B_2O_3–SiO_2 glass additive on densification and energy storage properties of $Ba_{0.4}Sr_{0.6}TiO_3$ ceramics, Journal of Materials Science: Materials in Electronics 23 (2012) 1599–1603.
[19] A. Tkach, P.M. Vilarinho, A. Senos, et al., Effect of nonstoichiometry on the microstructure and dielectric properties of strontium titanate ceramics, Journal of the European Ceramic Society 25 (2005) 2769–2772.
[20] Y.Y. Guo, H.M. Liu, D.P. Yu, et al., Ferroelectricity and superparamagnetism in Sr/Ti nonstoichiometric $SrTiO_3$, Physical Review B 85 (2012) 10410810.
[21] Y.S. Sung, J.M. Kim, J.H. Cho, et al., Effects of Bi nonstoichiometry in $(Bi_{0.5+x}Na)$ TiO_3 ceramics, Applied Physics Letters 98 (2011) 0129021.
[22] Y.S. Sung, J.M. Kim, J.H. Cho, et al., Effects of Na nonstoichiometry in $(Bi_{0.5}Na_{0.5+x})TiO_3$ ceramics, Applied Physics Letters 96 (2010) 0229012.
[23] R. Zuo, S. Su, Y. Wu, et al., Influence of A-site nonstoichiometry on sintering, microstructure and electrical properties of $(Bi_{0.5}Na_{0.5})TiO_3$ ceramics, Materials Chemistry and Physics 110 (2008) 311–315.